Available online at www.sciencedirect.com
ScienceDirect
Journal of Solid State Chemistry 180 (2007) 16–21
JOURNAL OF SOLID STATE CHEMISTRY
www.elsevier.com/locate/jssc

Synthesis, crystal structure and magnetic characterization of $Na_2Cu_5(Si_2O_7)_2$: An inorganic ferrimagnetic chain

António Moreira dos Santos[a,b,*], Paula Brandão[a], Andrew Fitch[c], Mário S. Reis[b], Vítor S. Amaral[b], João Rocha[a]

[a]*CICECO, Chemistry Department, University of Aveiro, Aveiro 3810-193, Portugal*
[b]*CICECO, Physics Department, University of Aveiro, Aveiro 3810-193, Portugal*
[c]*European Synchrotron Radiation Facility, Grenoble F-38043, France*

Received 4 July 2006; received in revised form 11 September 2006; accepted 12 September 2006
Available online 23 September 2006

Abstract

The hydrothermal synthesis, crystal structure and magnetic properties of the new copper silicate $Na_2Cu_5(Si_2O_7)_2$, are reported. The crystal structure was determined through synchrotron powder diffraction data. The unit cell was indexed to a triclinic cell, space group *P*-1 (n° 2) with unit cell parameters $a = 5.71075(2)$ Å, $b = 7.68266(3)$ Å, $c = 7.96742(3)$ Å, $\alpha = 64.2972(2)^\circ$, $\beta = 88.4860(2)^\circ$ and $\gamma = 70.5958(2)^\circ$ with $Z = 1$. A structural model was obtained through a combination of a direct-space Monte-Carlo approach and Rietveld refinement. The crystal structure contains parallel chains consisting of zig-zag copper dimers and trimers. All silicon atoms are present as part of a $[Si_2O_7]^{6-}$ anion that connects the chains; therefore the compound belongs to the sorosilicate mineral family. The magnetic susceptibility was measured and shows a behavior typical of one-dimensional ferrimagnetism, in agreement with the observed structure.

Keywords: Copper silicate; Structure determination from powder diffraction; Magnetic chain

1. Introduction

Low-dimensional magnetism has attracted much attention in recent years, due to its importance to fundamental physics research [1] and potential applications in spintronics [2]. Chain systems in particular, exhibit a variety of exotic properties, such as magnetic interaction alternation, [3] spin-Peierls transitions [4] or Haldane chains [5]. Many of these effects have been theoretically predicted and are now observed in real systems, which are often obtained through the use of innovative synthesis methods of new materials. The hydrothermal approach is one of such methods that operate far from thermodynamical equilibrium. Materials with a magnetic one-dimensional character, just as their three-dimensional counterparts, may exhibit ferro, [6] antiferro, [7] and ferrimagnetic ordering [8]. In general, the latter is achieved by incorporating two magnetic cations, with different *S* (be that different species or just different oxidation states) that couple antiferromagnetically, resulting in uncompensated spins. As far as one-dimensional magnetic systems are concerned, there are many examples of ferrimagnetism obtained through mixed metal coordination. Such magnetic behavior is more challenging to achieve in homo-metallic systems, because it requires a structure with either: (i) alternating metal sites along the chain, causing an alternation of the *g*-factor [9]; (ii) some level of clusterization of the chain with an odd number of metal centers, sometimes referred to as topological ferrimagnetism [10]; or (iii) a particular stacking of metal ions, like intertwined chains [11]. All of the homo-metallic ferrimagnetic chain structures reported to date (in which, each magnetic centre has only two nearest neighbors) have been metal-organic structures [12]. This occurs mainly due to the tunability afforded by metal-organic chemistry [13]. Purely inorganic examples of

*Corresponding author. Fax: +351 234 424985.
E-mail address: antonio@fis.ua.pt (A.M. dos Santos).

0022-4596/$ - see front matter © 2006 Elsevier Inc. All rights reserved.
doi:10.1016/j.jssc.2006.09.012

homo-metallic ferrimagnetic behavior are almost unknown, with the notable exception of the copper phosphate $Pb_3Cu_3(PO_4)_4$, whose magnetic behavior results from the stacking of Cu trimers [11]. Here we wish to report the synthesis, crystal structure determination from powder data and magnetic properties of $Na_2Cu_5(Si_2O_7)_2$, an unusual example of an inorganic ferrimagnetic chain.

2. Experimental

The synthesis of $Na_2Cu_5(Si_2O_7)_2$ was carried out in a Teflon-lined autoclave under static hydrothermal conditions. Typically, an alkaline solution was made by mixing 6.86 g sodium silicate solution (Na_2O 8 wt%, SiO_2 27 wt%, Merck), 7.37 g H_2O and 2.25 g NaOH (Panreac). A second solution was made by mixing 8.97 g H_2O with 1.80 g $CuSO_4 \cdot 5H_2O$ (Pronalab). These two solutions were combined and stirred thoroughly during 1 h. The gel with a molar composition 5.14 Na_2O:CuO:4.28 SiO_2:126.1 H_2O, was autoclaved for 7 days at 230 °C. The crystalline blue powder was filtered off, washed and dried overnight at 50 °C.

The chemical composition was determined with a Jobin-Yvon Induced Coupled Plasma JY-70. The obtained molar ratio Na:Cu:Si was 2.00:4.88:3.85, in agreement with the nominal composition 2:5:4 within 5% experimental error. Thermogravimetric analysis, performed on a Shimadzu TGA-50, showed no weight loss up to 700 °C.

For powder synchrotron diffraction studies, the sample was contained in a thin-walled borosilicate-glass capillary of diameter 0.5 mm and mounted on the high-resolution powder diffractometer ID31 at the ESRF Grenoble [14]. The sample was spun about its axis and the powder diffraction patterns were measured in the continuous-scanning mode at 2°/min 2θ, recording the data every 15 ms (0.0005° step in 2θ). The high-angle region was scanned several times to improve the statistics of these data. Measurements were made at 80 and 295 K, controlled by an Oxford Cryosystems Cryostream cooler. A wavelength of 0.80022(8) Å was selected using the liquid-nitrogen-cooled Si [111] double-crystal monochromator, and calibrated using a NIST 640c silicon standard. The data from the various scans and the nine detectors, each preceded by a Si [111] analyzer crystal, were normalized, combined and rebinned to a step of 0.002° 2θ [15] from 5° till 40° 2θ corresponding to 393 observed reflections for refinement. The magnetic susceptibility (M/H) was measured using a Oxford Instruments SQUID magnetometer, between 4 and 300 K, on a field-cooled sample, under an applied field of 100 Oe.

3. Results

Based on the metal ratios obtained through ICP chemical analysis and TGA measurements, showing that no water or OH groups are contained within the structure, the chemical composition was determined to be $Na_2Cu_5Si_4O_{14}$. The oxygen content was calculated assuming all copper is in the 2+ oxidation state, confirmed by the magnetic data (see below). A structural model was suggested by applying a real-space method implemented in the Fox [16] Suite, which is based on a Monte-Carlo optimization, against the theoretically generated powder pattern, of the arrangement of the contents of the unit cell. In order to reduce the number of free parameters in the optimization, one copper ion was fixed in the inversion center of the unit cell (0.5, 0.5, 0.5) since it contains an odd number of copper ions. In addition, assuming tetra-coordinated silicon, all the 14 oxygen ions should be part of the two Si_2O_7 units. These two assumptions were used in setting up the contents of the unit cell for the structure determination.

The first 20 reflections of the powder data were unambiguously indexed using the TREOR90 [17] software suite in PowderX [18] to a triclinic cell ($M20 = 20$; $F20 = 67$). Since the choice of space group in the triclinic system cannot be made based on systematic absences, statistical arguments and simplicity (the number of free parameters is reduced to almost half) were used to select $P\bar{1}$ since there are more structures in this space-group than in $P1$. The refined unit cell parameters are $a = 5.71075(2)$ Å, $b = 7.68266(3)$ Å, $c = 7.96742(3)$ Å, $\alpha = 64.2972(2)°$, $\beta = 88.4860(2)°$ and $\gamma = 70.5958(2)°$, unit cell volume of 294.20 Å^3, $Z = 1$, $\rho_{calc} = 3.95\,g\,cm^{-3}$. Further details of the crystal structure investigation(s) may be obtained from the Fachinformations-zentrum Karlsruhe, 76344 Eggenstein-Leopoldshafen, Germany (fax: (+49)7247-808-666; e-mail: crysdata@fiz-karlsruhe.de) on quoting the deposition number CSD-416179.

A summary of the crystal data, diffraction experiment parameters and refinement procedure is presented in Table 1. Rietveld refinement was used to optimize the atomic coordinates and profile parameters using the GSAS [19] suite (EXPGUI [20] interface). There were 72 free parameters in the final refinement; the isotropic thermal parameters for both Si atoms and seven oxygen atoms in the unit cell were constrained to be the same in the refinement. The peak profile function was a pseudo-Voigt with Stephens microstrain broadening. A plot of the measured diffraction, pattern together with the calculated one and the difference curve is shown in Fig. 1. The final quality of fit parameters were wRp = 0.10, Rp = 0.077 and $\chi^2 = 3.816$.

3.1. Crystal structure

The refined atomic coordinates and a selection of bond lengths and angles of the structure are shown in Tables 2 and 3, respectively, and an overview of the crystal structure is presented in Fig. 2(a). The structure of $Na_2Cu_5(Si_2O_7)_2$ is related to $Li_2Cu_5Si_4O_{14}$ [21]. All the three Cu^{2+} ions in the asymmetric unit are in square planar coordination with Cu–O bond lengths in the range 1.891–1.982 Å.The Cu–O connectivity, responsible for the magnetic properties, forms chains of alternating Cu_2O_6 dimers and Cu_3O_8 trimers

Table 1
Crystal data and experimental details for data collection and structure determination for $Na_2Cu_5(Si_2O_7)_2$

Crystal data	
Chemical formula	$Na_2Cu_5Si_4O_{14}$
Unit cell dimensions	
a, *b*, *c* (Å)	5.71075 (2), 7.68266 (3), 7.96742 (3)
α, β, γ (deg)	64.2972 (2), 88.4860 (2), 70.5958 (2)
Cell volume (Å^3)	294.20 (2)
Space group, *Z*	P-1, 1n
Calc. density (g/cm^{-3})	3.95
Colour	Blue
Synchrotron radiation	
λ (Å)	0.80022 (8)
Range (2θ)	5–40°
Increment (2θ)	0.002° (rebinned)
Observed reflections	390
Rietveld refinement	
Profile function	Pseudo-Voigt with Stephens microstrain broadening
Number of refined param.	72
w*R*p	0.10
*R*p	0.077
χ^2	3.816

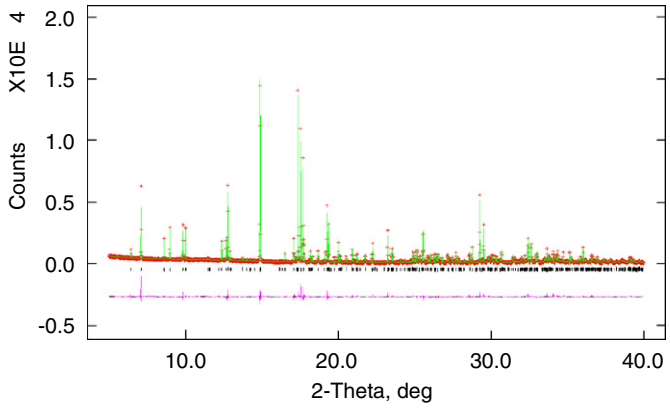

Fig. 1. Final refinement of $Na_2Cu_5(Si_2O_7)_2$, full range 5–40°, difference curve is plotted below the 2θ axis.

connected by O5, which lies slightly out of plane from the Cu clusters and with a Cu_2–O_5–Cu_3 angle of 119.5°, as shown in Fig. 3(a). The chain progresses in a zig-zag fashion, with an in-plane angle of ca. 60°. The largest deviation from planarity of the copper coordination is found in the dimer angle O_4–Cu_3–O_5 of 147.9°. At the end of the trimers, each Cu has an apical oxygen O_7 belonging to the basal plane of a copper belonging to a trimer unit of the chain above. This bond distance ($d_{Cu\text{-}O_7} = 2.707$ Å) is very large when compared with the square planar coordination. Similar Cu coordination was found in other Cu chain silicates and the long Cu–O bond was shown to be magnetically inactive, [22] not interfering with the magnetic network. These chains are separated in the plane by Si_2O_7 units (see text below).

The $Na_2Cu_5(Si_2O_7)_2$ structure belongs to the sorosilicate mineral class, since all silicon atoms are paired in Si_2O_7 double tetrahedra [Fig. 2b)]. The average Si–O bond length is 1.63 Å and the Si_1–O_1–Si_2 bond angle is 135.1°. All oxygen atoms in the structure except O_1 (connecting the two SiO_4 tetrahedra) are tri-coordinated to two coppers and one silicon atom. The six-coordinated sodium ion (Na–O bond lengths in the range 2.271–2.850 Å) is in a highly distorted six-coordination shown in Fig. 2(c) and lies in the plane of the chains, and may be viewed as the vertex of the kink in the chain.

Table 2
List of atomic coordinates for $Na_2Cu_5(Si_2O_7)_2$ and isotropical thermal parameters

Atom	Wycoff Site	*x*	*y*	*z*	U_{iso}
Cu1	1a	0.5	0.5	0.5	0.0057 (6)
Cu2	2i	0.1747 (2)	0.9277 (2)	0.2209 (2)	0.0069 (4)
Cu3	2i	0.5832 (2)	0.1020 (2)	0.3195 (2)	0.0063 (4)
Si1	2i	0.2345 (6)	0.6295 (5)	0.0518 (5)	0.0068 (1)
Si2	2i	0.9921 (5)	0.2617 (4)	0.3683 (3)	0.0068 (1)
Na1	2i	0.6954 (5)	0.7165 (4)	0.0956 (4)	0.002 (8)
O1	2i	0.9477 (9)	0.4979 (7)	0.2082 (6)	0.01 (2)
O2	2i	0.4897 (9)	0.7066 (7)	0.2449 (7)	0.01 (2)
O3	2i	0.5786 (9)	0.7029 (7)	−0.0733 (7)	0.01 (2)
O4	2i	1.2849 (9)	0.1478 (7)	0.4492 (7)	0.01 (2)
O5	2i	0.9058 (9)	0.1371 (8)	0.2673 (7)	0.01 (2)
O6	2i	0.8097 (9)	0.2789 (7)	0.5226 (7)	0.01 (2)
O7	2i	0.8121 (1)	0.8960 (8)	0.0360 (7)	0.01 (2)

3.2. Magnetic properties

At high temperatures, the susceptibility data (Fig. 4) reveals a typical Curie–Weiss behavior. The effective paramagnetic moment is 1.83 μ_B/Cu ion, a value close to the expected for an isolated copper ion in the 2+ oxidation state ($S = 1/2$). Below 125 K, there is a susceptibility increase, with respect to the predicted paramagnetic regime, characteristic of uncompensated spins at low-temperature. Finally, at ~8 K, a sharp peak in the susceptibility is observed (inset in Fig. 4), which is associated with the onset of an antiferromagnetic three-dimensional ground state.

For one-dimensional systems the χ_T plot versus temperature is often a more informative way to present the susceptibility data, and this is shown in Fig. 5. It shows a broad minimum in the 30–100 K range usually associated to ferrimagnetic low-dimensional systems [9,12,23].

In order to establish a magnetic interaction map from the analysis of the Cu–O connectivity, one can identify a chain topology, with a dimer–trimer alternation. That corresponds to two exchange interactions corresponding to each cluster J_{TR} (Cu_1–Cu_2 interaction, $d_{Cu_1-Cu_2} = 3.003$ Å) and J_D (Cu_3–Cu_3 interaction $d_{Cu_3-Cu_3} = 2.927$ Å) and one between clusters J_{DT} (Cu_2–Cu_3, $d_{Cu_2\text{-}Cu_3} = 3.404$ Å), as depicted in Fig. 3(b) confirming the chain character of this compound.

Some considerations about the magnetic structure of the chain can be inferred from the combination of the structural data and the measured magnetic data, by

Table 3
List of selected bond lengths and angles

Cu1–O2	1.949 (5)	Si1–O1	1.640 (5)	Na1–O1	2.271 (5)
Cu1–O2	1.949 (5)	Si1–O4	1.604 (5)	Na1–O2	2.516 (6)
Cu1–O6	1.949 (4)	Si1–O5	1.675 (5)	Na1–O3	2.306 (5)
Cu1–O6	1.949 (4)	Si1O6	1.611 (5)	Na1–O3	2.347 (5)
Cu2–O2	1.966 (5)	Si2–O1	1.690 (5)	Na1–O5	2.349 (6)
Cu2–O5	1.982 (5)	Si2–O2	1.646 (5)	Na1–O7	2.557 (5)
Cu2–O6	1.951 (5)	Si2–O3	1.575 (5)		
Cu2–O7	1.919 (5)	Si2–O7	1.611 (6)		
Cu3–O3	1.891 (5)				
Cu3–O4	1.979 (5)				
Cu3–O4	1.921 (5)				
Cu3–O5	1.958 (5)				
O2–Cu1–O2	180.0	O3–Cu3–O4	96.85 (2)	O2–Cu2–O5	162.99 (2)
O2–Cu1–O6	100.22 (2)	O3–Cu3–O4	163.14 (2)	O2–Cu2–O6	79.35 (2)
O2–Cu1–O6	79.78 (2)	O3–Cu3–O5	93.61 (2)	O2–Cu2–O7	94.06 (2)
O2–Cu1–O6	79.78 (2)	O4–Cu3–O4	82.78 (2)	O5–Cu2–O6	89.82 (2)
O2–Cu1–O6	100.22 (2)	O4–Cu3–O5	147.98 (2)	O5–Cu2-O7	97.12 (2)
O6–Cu1–O6	180.0	O4–Cu3–O5	95.50 (2)	O6–Cu2–O7	173.02 (2)
O1–Si1–O4	108.19 (3)	O1–Si2–O2	105.80 (3)		
O1–Si1–O5	108.75 (3)	O1–Si2–O3	107.45 (3)		
O1—Si1–O6	107.22 (3)	O1–Si2–O7	103.01 (3)		
O4–Si1–O5	109.55 (3)	Si1–O1–Si2	135.21 (3)		
O4-Si1-O6	114.75 (3)	O2-Si2–O3	106.60 (3)		
O5-Si1–O6	108.22 (3)	O2–Si2–O7	118.00 (3)		
O3–Si2–O7	115.09 (3)				

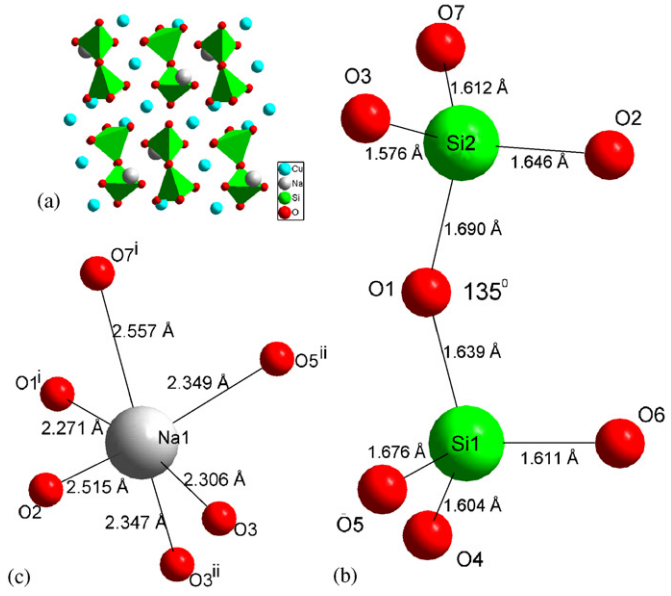

Fig. 2. Crystal structure of $Na_2Cu_5(Si_2O_7)_2$ (a) viewed along the 001 direction; (b) detail of the Si_2O_7 unit; (c) Distorted six-coordination environment of the Na ion. Symmetry operations used: (i) $-1+x, y, z$ and (ii) $1-x, 1-y, -z$.

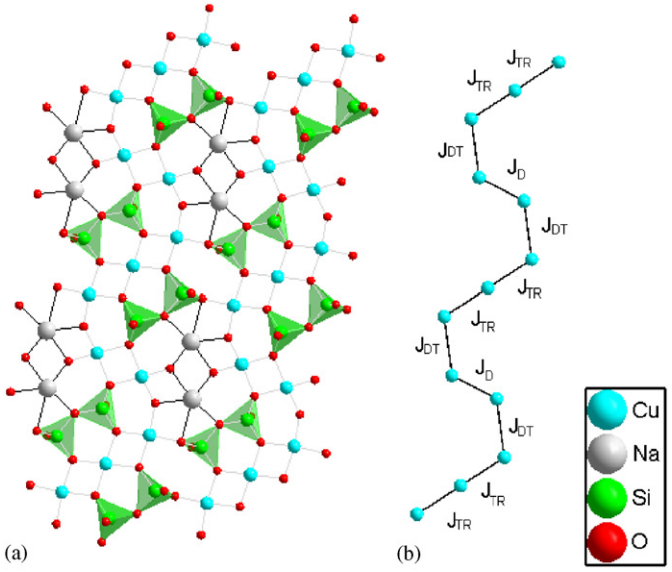

Fig. 3. Crystal structure of $Na_2Cu_5(Si_2O_7)_2$. (a) View of the plane containing the zig-zag Cu–O chains. (b) Magnetic exchange parameters along the Cu–O chains inferred from the structure, see text for details.

considering the high and low-temperature limits of the susceptibility:

In the low temperature limit we have

$$\lim_{T\to 0}(\gamma\chi T) = S(S+1) = 0.75, \quad (1)$$

where $\gamma = 3k/(g\mu_B)^2$ and S represents the net spin of the dimer–trimer repeat unit, which may assume three values: 5/2 (all interactions FM), 3/2 (for instance, intradimer AF and intratrimer FM) and 1/2 (for instance, dimer FM and trimer AF).

On the other hand, at high-temperature interactions between spins are negligible therefore:

$$\lim_{T\to\infty}(\gamma\chi T) = 5S_{Cu}(S_{Cu}+1) = 3.75, \quad (2)$$

where $S_{cu} = 1/2$ is the spin of an isolated Cu^{2+}.

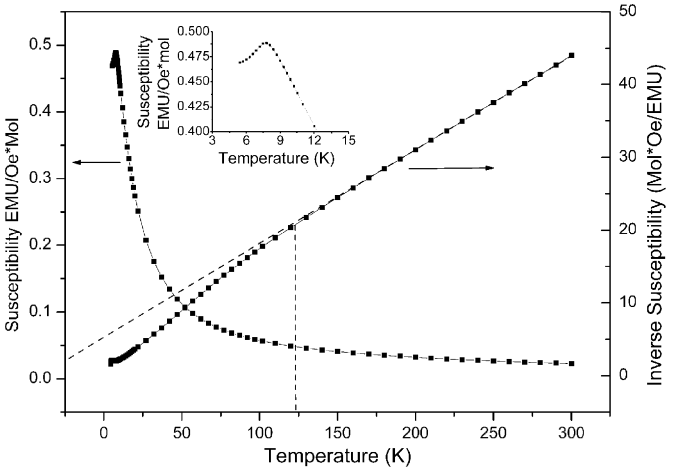

Fig. 4. Susceptibility data for $Na_2Cu_5(Si_2O_7)_2$. The right axis shows the inverse susceptibility, where the high-temperature linear region is evidence of the paramagnetic state with a negative θ_p. The inset shows the low-temperature transition to a three-dimensional antiferromagnetic ground state.

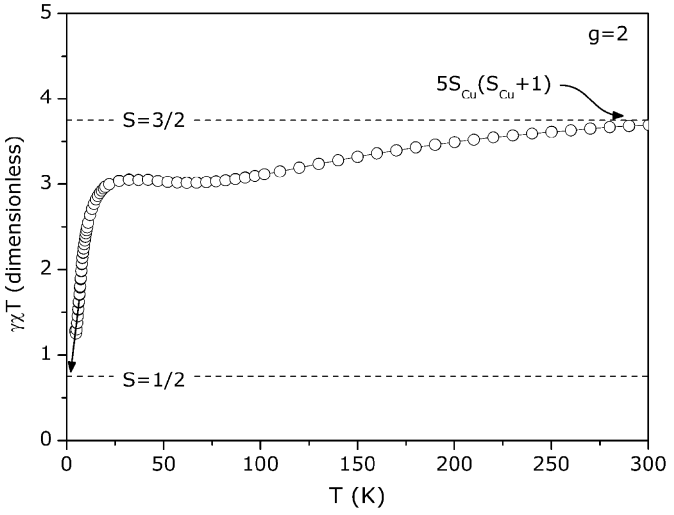

Fig. 5. $\gamma\chi$T plot normalized to $S(S+1)$ units on the vertical axis. The broad minimum between 30 and 100 K is associated to one-dimensional ferrimagnetism (see text). The high-temperature limit converges to the expected 5 Cu^{2+} ($S_{Cu} = 1/2$) isolated spins per chain repeat unit. The low-temperature limit tends to $S = 1/2$, where S represents the net spin of the ground state arrangement of the dimer-trimer pair. The γ parameter is a normalizing constant defined in the text. An approximate value of $g_{Cu} = 2$ was used in the calculations.

In Fig. 5 the theoretical high and low-temperature limits are plotted as horizontal lines. As expected, for high temperatures, the former tends towards the predicted value (Eq. (2)). For a ground state $S = 5/2$, Eq. (1) would take the value $5/2(5/2+1) = 8.75$ (horizontal line not shown for clarity) and, thus, may be excluded as a possibility. Between the two remaining options, ($S = 1/2$ or $3/2$) inspection of the χT plot shows clearly that the low-temperature limit is $S = 1/2$. We conclude therefore that the ground-state configuration of the dimer–trimer pair results in an uncompensated moment of $S = 1/2$.

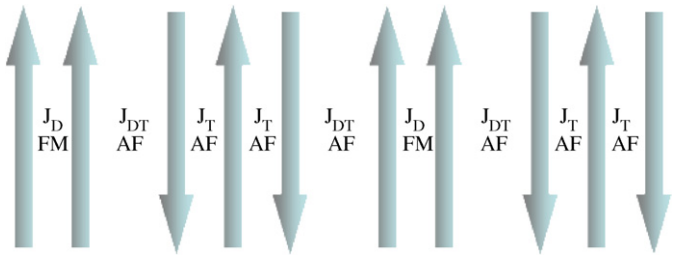

Scheme 1. Ferrimagnetic sequence of the magnetic interactions along the chain J_{TR} AF, J_D FM J_{DT} AF, from Ref. [24].

A magnetic Hamiltonian comprising the three magnetic interactions can be written as

$$H = -J_1 S_1 S_2 - J_1 S_2 S_3 - J_2 S_A S_B - J_3 S_4 S_5 - g\mu_B S_{Tot}. \quad (3)$$

Through the fit of this Hamiltonian to the magnetic data, it was possible to suggest a magnetic structure for the ferromagnetic chain, depicted in Scheme 1, and that is in agreement with the crystal structure presented here. A complete analysis of the Hamiltonian and the fitting procedure are discussed elsewhere.[24]

In conclusion, a new sorosilicate compound, $Na_2Cu_5(Si_2O_7)_2$, was synthesized and characterized. Its structure was determined through synchrotron powder diffraction and it contains unusual Cu–O zig-zag chains, of alternating dimers and trimers, and Si_2O_7 units. The magnetic susceptibility of this material is characteristic of one-dimensional ferrimagnetism, unprecedented among purely inorganic-chain systems.

Acknowledgments

António Moreira dos Santos and M. S. Reis wish to acknowledge FCT Grants BPD/14984/2004 and BPD/23184/2005 respectively. Work in Aveiro was performed under Project POCT/CTM/46780/02. The authors thank IFIMUP at the University of Porto for the SQUID measurements.

References

[1] D. Gatteschi, R. Sessoli, J. Magn. Magn. Mater. 272 (2004) 1030.
[2] (a) A.R. Rocha, V.M. Garcia-Suarez, S.W. Bailey, C.J. Lambert, J. Ferrer, S. Sanvito, Nat. Mater 4 (4) (2005) 335;
(b) V. Cerletti, W.A. Coish, O. Gywat, D. Loss, Nanotechnology 16 (4) (2005) R27.
[3] P. Brandão, F.A.A. Paz, J. Rocha, Chem. Comm. 2 (2005) 171.
[4] M. Hase, I. Terasaki, K. Uchinokura, Phys. Rev. Lett. 70 (23) (1993) 3651.
[5] W.J.L. Buyers, R.M. Morra, R.L. Armstrong, M.J. Hogan, P. Gerlach, K. Hirakawa, Phys. Rev. Lett. 4 (1986) 371.
[6] S. Dalai, P.S. Mukherjee, T. Mallah, M.G.B. Drew, N.R. Chaudhuri, Inorg. Chem. Comm. 7 (2002) 472.
[7] N. Motoyama, H. Eisaki, S. Uchida, Phys. Rev. Lett. 17 (1996) 3212.
[8] I.D. Watts, S.G. Carling, P.J. Day, Chem. Soc.-Dalton Trans. 7 (2002) 1429.

[9] E. Coronado, M. Drillon, P.R. Nugteren, L.J. Dejongh, D.J. Beltran, J. Am. Chem. Soc. 110 (12) (1988) 3907.
[10] A. Escuer, F.A. Mautner, M.A.S. Goher, M.A.M. Abu-Youssef, R. Vicente, Chem. Comm. 5 (2005) 605.
[11] M. Drillon, M. Belaiche, P. Legoll, J. Aride, A. Boukhari, A. Moquine, J Magn. Magn Mater. 128 (1–2) (1993) 83.
[12] S.J. Blundell, F.L. Pratt, J. Phys: Condens. Matt. 16 (24) (2004) R771.
[13] M.A.M. Abu-Youssef, A. Escuer, M.A.S. Goher, F.A. Mautner, G.J. Reiss, R. Vicente. Angew. Chem.- Int. Ed. 39 (9) (2000) 1624.
[14] A.N. Fitch, J. Res. Natl. Inst. Stand. Technol. 109 (2004) 133.
[15] J.P. Wright, G.B.M. Vaughan, A.N. Fitch, IUCr Comp. Commis. Newsletter 1 (2003) 92.
[16] V. Favre-Nicolin, R. Cerny, J. Appl. Crystallogr. 35 (Part 6) (2002) 734.
[17] P.E. Werner, L. Eriksson, M. Westdahl, J. Appl. Crystallogr. 18 (1985) 367.
[18] C. Dong, J. Appl. Crystallogr. 32 (1999) 838.
[19] A.C. Larson, R.B. Von Dreele, "General Structure Analysis System (GSAS)". Los Alamos National Laboratory Report LAUR 86-748 (1994).
[20] B.H. Toby, J. Appl. Crystallogr. 34 (2001) 210.
[21] K. Kawamura, A. Kawahara, J.T. Iiyama, Acta Crystallogr. Sect. B Struct. Sci. 34 (1978) 3181.
[22] A. Moreira dos Santos, V.S. Amaral, P. Brandao, F.A.A. Paz, J. Rocha, L.P. Ferreira, M. Godinho, O. Volkova, A. Vasiliev, Phys. Rev. B 72 (9) (2005) 092403.
[23] (a) M. Drillon, E. Coronado, M. Belaiche, R.L. Carlin, J. Appl. Phys. 63 (8 Part 2) (1988) 3551;
(b) E. Coronado, F. Sapina, M. Drillon, L.J. Dejongh, J. Appl. Phys 67 (9 Part 2B) (1990) 6001.
[24] M.S. Reis, A.M. dos Santos, V.S. Amaral, P. Brandão, J. Rocha, Phys. Rev. B 73 (2006) 214415.